Available online at www.sciencedirect.com
SCIENCE DIRECT®
Journal of Sound and Vibration 293 (2006) 138–155
JOURNAL OF SOUND AND VIBRATION
www.elsevier.com/locate/jsvi

Evidences of global bifurcations of an imperfect circular plate

M.H. Yeo[a], W.K. Lee*

[a]Display Division R&D Laboratory, LG Electronics Inc., Gumi 703-727, Republic of Korea
[b]School of Mechanical Engineering, Yeungnam University, Gyongsan 712-749, Republic of Korea

Received 3 August 2004; received in revised form 10 March 2005; accepted 25 September 2005
Available online 10 January 2006

Abstract

The global bifurcations in modal interactions of an imperfect circular plate with one-to-one internal resonance are investigated. The case of the third-order subharmonic resonance, in which an excitation frequency is near triple natural frequencies, is considered. The equations governing nonlinear oscillations of an imperfect circular plate are reduced to a system of non-autonomous ordinary differential equations via Galerkin's procedure. The method of multiple scales is used to obtain a system of autonomous ordinary differential equations, and then Kovačič and Wiggins' method is used to investigate the global dynamics of the plate. Having found a sufficient condition under which Silnikov-type homoclinic orbit can exist, we failed to observe any numerical evidences of global bifurcation.

1. Introduction

A plate experiences mid-plane stretching when deflected. The influence of this stretching on the dynamic response increases with the amplitude of the response. This situation can be described by nonlinear strain–displacement equations and a linear stress–strain law which give us the dynamic analogue of the von Karman equations with geometric nonlinearity. Modal interactions in nonlinear dynamic responses of a plate subjected to harmonic excitations have been investigated in two directions. The one is to investigate local bifurcations and the other global bifurcations. Local bifurcations are concerned with bifurcations of fixed points of vector fields and maps. Global bifurcations are about a qualitative change in the orbit structure of an extended region of phase space. Homoclinic and heteroclinic bifurcations are typical examples of global bifurcations [1].

For local bifurcations, modal interactions of rectangular plates with one-to-one internal resonance have been studied by many researchers including Chang et al. [2]. Many works on modal interactions of perfect or imperfect, circular plates have been done since Efstathiades [3] derived the equations governing the free, undamped oscillations of non-uniform, circular plates. Sridhar et al. [4] and Hadian and Nayfeh [5] studied symmetric responses in primary resonance of a circular plate with three-mode interaction. Lee and Kim [6] studied combination resonances of the plate. Sridhar et al. [7] derived solvability conditions for asymmetric responses of a circular plate. Nayfeh and Vakakis [8] found subharmonic traveling waves in a circular plate.

*Corresponding author.
E-mail addresses: yeomh@lge.com (M.H. Yeo), wklee@yu.ac.kr (W.K. Lee).

0022-460X/$ - see front matter © 2005 Elsevier Ltd. All rights reserved.
doi:10.1016/j.jsv.2005.09.035

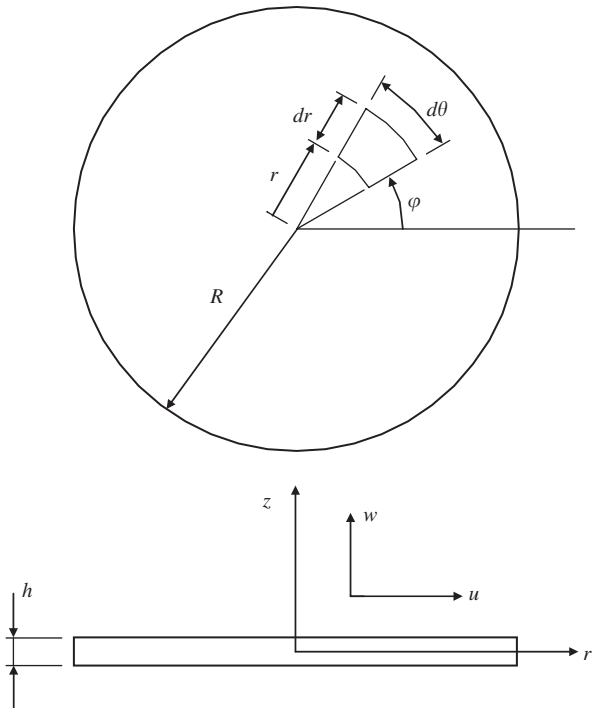

Fig. 1. A schematic diagram of a circular plate.

Yeo and Lee [9] found that solvability conditions by Sridhar et al. [7] were misderived, and corrected the conditions. Using the corrected solvability conditions, Lee and Yeo [10] investigated modal interactions of a circular plate on an elastic foundation, with one-to-three internal resonance. Lee et al. [11] studied the effect of the number of nodal diameters on the interactions of the plate. Contrary to works on perfect circular plates [4–11], Touzé et al. [12] and Thomas et al. [13], respectively, investigated theoretically and experimentally modal interactions of imperfect circular plates with free edge.

Study of global bifurcations in modal interactions of rectangular plates with one-to-one internal resonance had been initiated by Sethna and his colleagues [14–16]. Using the Melnikov method, they observed that breaking of heteroclinic orbits of a dynamical system governing a nearly square plate leads to Smale horseshoes leading chaos. Kovačič and Wiggins [17] developed global perturbation techniques for detecting homoclinic and heteroclinic orbits in a class of four-dimensional ordinary differential equations that are perturbations of two-degree-of-freedom Hamiltonian systems. Combining the higher dimensional Melnikov theory with geometrical singular perturbation theory and the theory of foliations of invariant manifolds, they obtained a sufficient condition for the existence of Silnikov-type homoclinic orbits. Their method has been applied to several problems including rectangular plates [18–22].

Since global bifurcations of circular plate have not been studied, in this paper we investigate global bifurcations in modal interactions of an imperfect circular plate shown in Fig. 1, with one-to-one internal resonance. The case of the third-order subharmonic resonance, in which an excitation frequency is near triple natural frequencies, is considered. The equations governing nonlinear oscillations of imperfect circular plates are reduced to a system of non-autonomous ordinary differential equations via Galerkin's procedure. The method of multiple scales is used to obtain a system of autonomous ordinary differential equations, and then Kovačič and Wiggins' method is used to investigate the global dynamics of the plate.

2. Formulation of the problem

The equations governing the free, undamped oscillations of non-uniform circular plates were derived by Efstathiades [3]. Damping and forcing terms are added, then the non-dimensionalized equations of motion of

an imperfect circular plate shown in Fig. 1 can be given as follows:

$$\rho h \frac{\partial^2 w}{\partial t^2} + \nabla^2(D\nabla^2 w) = (1-v)L_1(w,D) + L_2(w,F) - \frac{\delta}{2}\frac{\partial w}{\partial t} + p(r,\theta,t), \tag{1a}$$

$$\nabla^2(S\nabla^2 F) = (1+v)L_3(F,S) + \left(\frac{1}{r}\frac{\partial^2 w}{\partial r\,\partial\theta} - \frac{1}{r^2}\frac{\partial w}{\partial\theta}\right)^2 - \frac{\partial^2 w}{\partial r^2}\left(\frac{1}{r}\frac{\partial w}{\partial r} + \frac{1}{r^2}\frac{\partial^2 w}{\partial\theta^2}\right), \tag{1b}$$

where

$$L_1(w,D) = \frac{\partial^2 D}{\partial r^2}\left(\frac{1}{r}\frac{\partial w}{\partial r} + \frac{1}{r^2}\frac{\partial^2 w}{\partial\theta^2}\right) + \frac{\partial^2 w}{\partial r^2}\left(\frac{1}{r}\frac{\partial D}{\partial r} + \frac{1}{r^2}\frac{\partial^2 D}{\partial\theta^2}\right) - 2\left(\frac{1}{r}\frac{\partial^2 D}{\partial r\,\partial\theta} - \frac{1}{r^2}\frac{\partial D}{\partial\theta}\right)\left(\frac{1}{r}\frac{\partial^2 w}{\partial r\,\partial\theta} - \frac{1}{r^2}\frac{\partial w}{\partial\theta}\right),$$

$$L_2(w,F) = \frac{\partial^2 w}{\partial r^2}\left(\frac{1}{r}\frac{\partial F}{\partial r} + \frac{1}{r^2}\frac{\partial^2 F}{\partial\theta^2}\right) + \frac{\partial^2 F}{\partial r^2}\left(\frac{1}{r}\frac{\partial w}{\partial r} + \frac{1}{r^2}\frac{\partial^2 w}{\partial\theta^2}\right) - 2\left(\frac{1}{r}\frac{\partial^2 F}{\partial r\,\partial\theta} - \frac{1}{r^2}\frac{\partial F}{\partial\theta}\right)\left(\frac{1}{r}\frac{\partial^2 w}{\partial r\,\partial\theta} - \frac{1}{r^2}\frac{\partial w}{\partial\theta}\right),$$

$$L_3(F,S) = \frac{\partial^2 S}{\partial r^2}\left(\frac{1}{r}\frac{\partial F}{\partial r} + \frac{1}{r^2}\frac{\partial^2 F}{\partial\theta^2}\right) + \frac{\partial^2 F}{\partial r^2}\left(\frac{1}{r}\frac{\partial S}{\partial r} + \frac{1}{r^2}\frac{\partial^2 S}{\partial\theta^2}\right) - 2\left(\frac{1}{r}\frac{\partial^2 S}{\partial r\,\partial\theta} - \frac{1}{r^2}\frac{\partial S}{\partial\theta}\right)\left(\frac{1}{r}\frac{\partial^2 F}{\partial r\partial\theta} - \frac{1}{r^2}\frac{\partial F}{\partial\theta}\right),$$

F is the force function which satisfies the in-plane equilibrium conditions (in-plane inertia is neglected), and $w = w_0/z_0$ is the non-dimensional deflection in the middle surface, where w_0 is the deflection of middle surface and z_0 is the thickness at centre. $r = r_0/R$ is the non-dimensional radial coordinate, where r_0 is the radial coordinate and R is the radius of the plate. θ is angular coordinate and $p(r,\theta,t)$ is the forcing function. $D = D_0/E_0 z_0^3$ is the non-dimensional flexural rigidity, where $D_0 = Eh_0^3/12(1-v^2)$ is the flexural rigidity which is defined by Young's modulus, E, the thickness, h_0, Poisson's ratio,v, and Young's modulus at center, E_0. $S = E_0 z_0/Eh_0$ is a non-dimensional function, $\rho = \rho_0 R^4/E_0 z_0$ is a parameter proportional to the density, ρ_0, and

$$\nabla^4 = \nabla^2\nabla^2, \quad \nabla^2 = \frac{\partial^2}{\partial r^2} + \frac{1}{r}\frac{\partial}{\partial r} + \frac{1}{r^2}\frac{\partial^2}{\partial\theta^2}.$$

The relationships between F, w and the in-plane displacements, u_r and u_θ, are given by

$$e_r = S\left(\frac{1}{r}\frac{\partial F}{\partial r} + \frac{1}{r^2}\frac{\partial^2 F}{\partial\theta^2} - v\frac{\partial^2 F}{\partial r^2}\right), \quad e_\theta = S\left[\frac{\partial^2 F}{\partial r^2} - v\left(\frac{1}{r}\frac{\partial F}{\partial\theta} + \frac{1}{r}\frac{\partial^2 F}{\partial r\,\partial\theta}\right)\right], \tag{2a,b}$$

$$e_{r\theta} = 2S(1+v)\left(\frac{1}{r^2}\frac{\partial F}{\partial\theta} - \frac{1}{r}\frac{\partial^2 F}{\partial r\,\partial\theta}\right), \tag{2c}$$

where

$$e_r = \frac{\partial u_r}{\partial r} + \frac{1}{r}\left(\frac{\partial w}{\partial r}\right)^2, \quad e_\theta = \frac{u_r}{r} + \frac{1}{r}\frac{\partial u_\theta}{\partial\theta} + \frac{1}{2r^2}\left(\frac{\partial w}{\partial\theta}\right)^2,$$

$$e_{r\theta} = \frac{1}{r}\frac{\partial u_r}{\partial r} + \frac{\partial u_\theta}{\partial r} - \frac{u_\theta}{r} + \frac{1}{r}\frac{\partial w}{\partial r}\frac{\partial w}{\partial\theta}.$$

For plates which are nominally homogeneous and nominally flat it will be assumed that the small variation of S will not greatly affect the value of the force function F. Thus S is taken as constant (≈ 1) in Eqs. (1)

and (2). We assume that D and δ are functions of r, and ρh is a function of r and θ. Then the imperfection of the plate is due to the variation of ρh with θ.

It is well known [3,8] that perfect circular plates possess pairs of degenerate modes with equal natural frequencies and mode shapes with the same number of nodal lines. In reality, because of inevitable small imperfections, it has been shown that such modes have slightly different modal frequencies and that one configuration is moderately rotated with respect to the other, so that the degeneracy is broken [3,12,13].

We are, in this study, interested in motions when the plate is harmonically excited. In order to investigate the so-called third-order sub-harmonic resonance, we consider the case that the natural frequencies of two modes involved are near one-third of the excitation frequency. The interactions of two modes having slightly different frequencies, generated from the breaking of degeneracy, are considered. Then, the steady-state solution in Eqs. (1) and (2) can be approximated to [3]

$$w(r,\theta,t) = \phi(r)[x_1(t)\cos(n\theta-\theta_0)+x_2(t)\sin(n\theta-\theta_0)], \tag{3}$$

where $\phi(r)$ is the shape function which is determined by boundary conditions, and $x_1(t)$ and $x_2(t)$ are called coordinates of cosine and sine modes, respectively. The deflection of plate w implies a standing wave when either coordinate is zero, and a traveling wave when both coordinates are non-zero. n is the number of nodal diameters. θ_0 is caused by the imperfections of the plate and is a constant defined by the form of ρh as follows:

$$\theta_0 = \frac{1}{2}\tan^{-1}\frac{2A_0}{A_{11}-A_{21}}, \tag{4}$$

where

$$A_{11} = \int_0^{2\pi}\int_0^1 \rho h\phi^2 r\cos^2 n\theta\,\mathrm{d}r\,\mathrm{d}\theta, \quad A_{21} = \int_0^{2\pi}\int_0^1 \rho h\phi^2 r\sin^2 n\theta\,\mathrm{d}r\,\mathrm{d}\theta, \tag{5a,b}$$

$$A_0 = \frac{1}{2}\int_0^{2\pi}\int_0^1 \rho h\phi^2 r\sin 2n\theta\,\mathrm{d}r\,\mathrm{d}\theta. \tag{5c}$$

The angle θ_0 determines the position of the nodal diameters. In the case of perfection (ρh is the function of r only), the positions of nodal diameters are arbitrary because $A_0 = 0$ and $A_{11} = A_{21}$ in Eq. (4).

When both ρh and D are functions of θ, two θ_0's in Eq. (3) become distinct. Thus, the nodal diameters of two modes do not lie symmetrically [3].

Using Galerkin's procedure in Eq. (3), we obtain a system of non-autonomous ordinary differential equations as follows [3]:

$$\ddot{x}_i + \varepsilon\delta\omega_i^2\dot{x}_i + \omega_i^2 x_i + \varepsilon\gamma\omega_i^2 x_i(x_1^2+x_2^2) = \mu_i\cos\lambda t, \quad i=1,2, \tag{6}$$

where $\cdot = \mathrm{d}/\mathrm{d}t$ and ε is a small parameter. ω_i, δ, γ and μ_i are defined as follows:

$$\omega_i^2 = \frac{C_i}{M}, \quad \varepsilon\delta = \frac{F_{11}}{K_{11}}, \quad \varepsilon\gamma = \frac{B_0}{K_{11}}, \quad \mu_i = \frac{N_i}{M}, \quad i=1,2, \tag{7}$$

where

$$C_1 = K_{11}(A_{11}\tan^2\theta_0 - 2A_0\tan\theta_0 + A_{21}),$$

$$C_2 = K_{11}(A_{21}\tan^2\theta_0 + 2A_0\tan\theta_0 + A_{11}),$$

$$N_1 = \sec\theta_0\{A_{21}P_1 - A_0P_2 - (A_0P_1 - A_{11}P_2)\tan\theta_0\},$$

$$N_2 = \sec\theta_0\{A_{11}P_2 - A_0P_1 + (A_0P_2 - A_{21}P_1)\tan\theta_0\},$$

$$M = (A_{11}A_{21} - A_0^2)(1+\tan^2\theta_0),$$

$$P_1 = \int_0^{2\pi}\int_0^1 p^*(r,\theta)\phi r\cos n\theta\,\mathrm{d}r\,\mathrm{d}\theta, \quad P_2 = \int_0^{2\pi}\int_0^1 p^*(r,\theta)\phi r\sin n\theta\,\mathrm{d}r\,\mathrm{d}\theta,$$

$$K_{11} = -\pi \int_0^1 \bar{A}_1 \phi r \, \mathrm{d}r, \quad F_{11} = \pi \int_0^1 c\phi^2 r \mathrm{d}r, \quad B_0 = -\frac{\pi}{4} \int_0^{2\pi} \phi(2\bar{A}_2 + \bar{A}_3 - \bar{B}_2) r \, \mathrm{d}r. \tag{8}$$

$\bar{A}_1$, $\bar{A}_2$, $\bar{A}_3$ and $\bar{B}_2$ are determined by n, r, v, ϕ, and the shape function of F [3].

In order for system (6) to have the characteristic of hardening spring, we assume that γ is positive. And we consider the harmonic excitation $p(r, \theta, t) = p^*(r, \theta) \cos \lambda t$.

In system (6), we assume that $\mu_1 = 0$. Since $\mu_1 = 0$ means $N_1 = 0$, P_1 and P_2 must satisfy the relation

$$(A_0 - A_{11} \tan \theta_0) P_2 = (A_{21} - A_0 \tan \theta_0) P_1. \tag{9}$$

Then we have

$$\mu_2 = \frac{N_2}{M} = \frac{P_1 \sec \theta_0}{A_0 - A_{11} \tan \theta_0} \quad \text{or} \quad \frac{P_2 \sec \theta_0}{A_{21} - A_0 \tan \theta_0}. \tag{10,11}$$

Noting $\omega_1 \approx \omega_2$ (due to breaking of degeneracy) and $\lambda/3 \approx \omega_i$ (due to third-order sub-harmonic resonance), we introduce two detuning parameters β and σ as follows:

$$\omega_2 = \omega_1 + \varepsilon\beta, \quad \lambda = 3\omega_2 + \varepsilon\sigma. \tag{12a,b}$$

In order to use the method of multiple scales we assume

$$x_i(t) = x_{i0}(T_0, T_1) + \varepsilon x_{i1}(T_0, T_1) + O(\varepsilon^2), \tag{13}$$

where $T_i = \varepsilon^i t$, $i = 0, 1$. Substituting Eq. (13) into Eq. (6) and equating coefficients of like powers of ε yield

$O(1)$:

$$D_0^2 x_{10} + \omega_1^2 x_{10} = 0, \quad D_0^2 x_{20} + \omega_2^2 x_{20} = \mu_2 \cos \lambda T_0. \tag{14a,b}$$

$O(\varepsilon)$:

$$D_0^2 x_{11} + \omega_1^2 x_{11} = -2D_0 D_1 x_{10} - \delta\omega_1^2 D_0 x_{10} - \gamma\omega_1^2 (x_{10}^3 + x_{10} x_{20}^2), \tag{15a}$$

$$D_0^2 x_{21} + \omega_2^2 x_{21} = -2D_0 D_1 x_{20} - \delta\omega_2^2 D_0 x_{20} - \gamma\omega_2^2 (x_{20}^3 + x_{20} x_{10}^2). \tag{15b}$$

The general solution of Eq. (14) can be written in the form

$$x_{10} = A_1(T_1) \exp(\mathrm{i}\omega_1 T_0) + \mathrm{cc}, \quad x_{20} = A_2(T_1) \exp(\mathrm{i}\omega_2 T_0) + \Lambda \exp(\mathrm{i}\lambda T_0) + \mathrm{cc}, \tag{16a,b}$$

where $\Lambda = \mu_2/2(\omega_2^2 - \lambda^2)$ and cc represents the complex conjugate of the preceding term. The functions $A_1(T_1)$ and $A_2(T_1)$ are to be determined by satisfying the solvability conditions for boundedness of the solution. Term $\Lambda \exp(\mathrm{i}\lambda T_0)$ will give the non-resonance response [6,23]. Substituting Eq. (16) into Eq. (15) and using Eq. (12), we obtain solvability conditions as follows:

$$\begin{aligned} &\mathrm{i}(2A_1' + \delta\omega_1^2 A_1) + \gamma\omega_1 \{A_1(3|A_1|^2 + 2|A_2|^2 + 2\Lambda^2) \\ &\quad + \bar{A}_1 A_2^2 \exp[2\mathrm{i}\beta T_1] + 2\Lambda \bar{A}_1 \bar{A}_2 \exp[\mathrm{i}(2\beta + \sigma) T_1]\} = 0, \end{aligned} \tag{17a}$$

$$\begin{aligned} &\mathrm{i}(2A_2' + \delta\omega_2^2 A_2) + \gamma\omega_2 \{A_2(2|A_1|^2 + 3|A_2|^2 + 6\Lambda^2) \\ &\quad + A_1^2 \bar{A}_2 \exp[-2\mathrm{i}\beta T_1] + \Lambda \bar{A}_1^2 \exp[\mathrm{i}(2\beta + \sigma) T_1] + 3\Lambda \bar{A}_2^2 \exp[\mathrm{i}\sigma T_1]\} = 0, \end{aligned} \tag{17b}$$

where a prime denotes differentiation with respect to the slow time T_1 and $\bar{A}_n$ denotes the complex conjugate of A_n. Next we let

$$A_i = \sqrt{2a_i} \exp[\mathrm{i}\hat{\varphi}_i], \quad i = 1, 2, \tag{18}$$

where a_i and $\hat{\varphi}_i$ are the real functions of T_1. Substituting Eq. (18) into (17) and separating the result into real and imaginary parts yields

$$a_1' = -\delta\omega_1^2 a_1 + 2\gamma\omega_1 a_1 \{a_2 \sin 2(\varphi_1 - \varphi_2) + \sqrt{2}\Lambda\sqrt{a_2} \sin(2\varphi_1 + \varphi_2)\}, \tag{19a}$$

$$\varphi_1' = -\beta - \frac{\sigma}{3} + \gamma\omega_1\{3a_1 + 2a_2 + \Lambda^2 + a_2\cos 2(\varphi_1 - \varphi_2) + \sqrt{2}\Lambda\sqrt{a_2}\cos(2\varphi_1 + \varphi_2)\}, \tag{19b}$$

$$a_2' = -\delta\omega_2^2 a_2 - \gamma\omega_2\{2a_1a_2\sin 2(\varphi_1 - \varphi_2) - \sqrt{2}\Lambda a_1\sqrt{a_2}\sin(2\varphi_1 + \varphi_2) - 3\sqrt{2}\Lambda a_2\sqrt{a_2}\sin 3\varphi_2\}, \tag{19c}$$

$$\varphi_2' = -\frac{\sigma}{3} + \gamma\omega_2\left\{(2a_1 + 3a_2 + 3\Lambda^2) + a_1\cos 2(\varphi_1 - \varphi_2) + \frac{\Lambda a_1}{\sqrt{2}\sqrt{a_2}}\cos(2\varphi_1 + \varphi_2) + \frac{3\Lambda}{\sqrt{2}}\sqrt{a_2}\cos 3\varphi_2\right\}, \tag{19d}$$

where $\varphi_1 = \hat{\varphi}_1 - (\beta + \sigma/3)T_1$ and $\varphi_2 = \hat{\varphi}_2 - (\sigma/3)T_1$.

In order to apply the perturbation method given by Kovačič and Wiggins [17] we consider the following canonical transformation to bring system (19) to the appropriate form

$$q_1 = \varphi_1 - \varphi_2, \quad q_2 = \varphi_2, \quad p_1 = a_1, \quad p_2 = a_1 + a_2. \tag{20}$$

This transformation leads to the following set of a equations in (p_1, q_1,p_2,q_2) coordinates:

$$\begin{aligned}\dot{p}_1 &= 2p_1(p_2 - p_1)\sin 2q_1 \\ &\quad + 2\varepsilon p_1[-c - \gamma b(p_2 - p_1)\sin 2q_1 + \sqrt{2}f\sqrt{p_2 - p_1}\sin(2q_1 + 3q_2)] + O(\varepsilon^2) \\ &= -\frac{\partial H}{\partial q_1} + 2\varepsilon p_1[-c - \gamma b(p_2 - p_1)\sin 2q_1] + O(\varepsilon^2),\end{aligned} \tag{21a}$$

$$\begin{aligned}\dot{q}_1 &= -b + (2p_1 - p_2)(1 - \cos 2q_1) + \varepsilon\left[-\gamma b(p_1 + 2p_2) - \gamma b(p_2 - p_1)\cos 2q_1 - \frac{3}{\sqrt{2}}f\sqrt{p_2 - p_1}\cos 3q_2 + \frac{f(2p_2 - 3p_1)}{\sqrt{2}\sqrt{p_2 - p_1}}\cos(2q_1 + 3q_2)\right] + O(\varepsilon^2) \\ &= \frac{\partial H}{\partial p_1} + \varepsilon[-\gamma b(p_1 + 2p_2) - \gamma b(p_2 - p_1)\cos 2q_1] + O(\varepsilon^2),\end{aligned} \tag{21b}$$

$$\begin{aligned}\dot{p}_2 &= \varepsilon[-2cp_2 - 2\gamma b p_1(p_2 - p_1)\sin 2q_1 \\ &\quad + 3\sqrt{2}f(p_2 - p_1)^{3/2}\sin 3q_2 + 3\sqrt{2}fp_1\sqrt{p_2 - p_1}\sin(2q_1 + 3q_2)] + O(\varepsilon^2) \\ &= -\frac{\partial H}{\partial q_2} + \varepsilon[-2cp_2 - 2\gamma b p_1(p_2 - p_1)\sin 2q_1] + O(\varepsilon^2),\end{aligned} \tag{21c}$$

$$\begin{aligned}\dot{q}_2 &= -p_1 + 3p_2 - s + p_1\cos 2q_1 \\ &\quad + \varepsilon\left[\frac{3f}{\sqrt{2}}\sqrt{p_2 - p_1}\cos 3q_2 + \frac{fp_1\cos(2q_1 + 3q_2)}{\sqrt{2}\sqrt{p_2 - p_1}}\right] + O(\varepsilon^2) \\ &= \frac{\partial H}{\partial p_2} + O(\varepsilon^2),\end{aligned} \tag{21d}$$

where

$$\varepsilon c = \delta\omega_2/2\gamma, \quad \varepsilon f = \Lambda, \quad b = \beta/\gamma\omega_2, \quad s = \sigma/3\gamma\omega_2, \quad \tau = \gamma\omega_2 T_1. \tag{22}$$

In Eq. (21) a dot denotes the differentiation with respect to τ. The Hamiltonian function H is given as follows:

$$H(p_1, q_1, p_2, q_2) = H_0(p_1, q_1, p_2, q_2) + \varepsilon H_1(p_1, q_1, p_2, q_2), \tag{23}$$

where

$$H_0(p_1,q_1,p_2,q_2) = -bp_1 + \frac{3}{2}p_2^2 - sp_2 - p_1(p_2-p_1)(1-\cos 2q_1), \tag{24a}$$

$$H_1(p_1,q_1,p_2,q_2) = \sqrt{2}f\sqrt{p_2-p_1}\,[(p_2-p_1)\cos 3q_2 + p_1\cos(2q_1+3q_2)]. \tag{24b}$$

Observing that the coordinate system (p_1, q_1,p_2,q_2) is singular at $p_1 = 0$, we introduce the following canonical transformation in order to avoid the singular behavior. We will soon see that the fixed points at $p_1 = 0$ play an important role in defining the dynamics of our system:

$$x = \sqrt{2p_1}\cos q_1, \quad y = \sqrt{2p_1}\sin q_1, \quad I = p_2, \quad \varphi = q_2. \tag{25}$$

It is observed that in view of Eqs. (20) and (25) when cosine mode ($x_1(t)$) vanishes, $x = y = 0$ and I becomes a_2, amplitude of sine mode ($x_2(t)$).

Eq. (21), H_0 and H_1 are expressed as follows:

$$\dot{x} = y(b + 2I - x^2 - 2y^2) + \varepsilon g^x + O(\varepsilon^2) = -\frac{\partial H_0}{\partial y} + \varepsilon g^x + O(\varepsilon^2), \tag{26a}$$

$$\dot{y} = x(-b + y^2) + \varepsilon g^y + O(\varepsilon^2) = \frac{\partial H_0}{\partial x} + \varepsilon g^y + O(\varepsilon^2), \tag{26b}$$

$$\dot{I} = \varepsilon g^I + O(\varepsilon^2) = -\frac{\partial H_0}{\partial \varphi} + \varepsilon g^I + O(\varepsilon^2), \tag{26c}$$

$$\dot{\varphi} = 3I - s - y^2 + \varepsilon g^\varphi + O(\varepsilon^2) = \frac{\partial H_0}{\partial I} + \varepsilon g^\varphi + O(\varepsilon^2), \tag{26d}$$

where

$$\begin{aligned} g^x =& -cx + \gamma by(I + x^2 + y^2) \\ &+ \frac{fx(2I - x^2 - 2y^2)}{\sqrt{2I - x^2 - y^2}}\sin 3\varphi + \frac{fy(5I - 2x^2 - 3y^2)}{\sqrt{2I - x^2 - y^2}}\cos 3\varphi \\ =& -\frac{\partial H_1}{\partial y} - cx + \gamma by(I + x^2 + y^2), \end{aligned} \tag{27a}$$

$$\begin{aligned} g^y =& -cy - 3\gamma bxI - \frac{fx(I - y^2)}{\sqrt{2I - x^2 - y^2}}\cos 3\varphi - \frac{fy(2I - 2x^2 - y^2)}{\sqrt{2I - x^2 - y^2}}\sin 3\varphi \\ =& \frac{\partial H_1}{\partial x} - cy - 3\gamma bxI, \end{aligned} \tag{27b}$$

$$\begin{aligned} g^I =& -2cI - \gamma bxy(2I - x^2 - y^2) + 3fxy\sqrt{2I - x^2 - y^2}\cos 3\varphi \\ &+ 3f(I - y^2)\sqrt{2I - x^2 - y^2}\sin 3\varphi \\ =& -\frac{\partial H_1}{\partial \varphi} - 2cI - \gamma bxy(2I - x^2 - y^2), \end{aligned} \tag{27c}$$

$$g^\varphi = \frac{f(3I - x^2 - 2y^2)\cos 3\varphi}{\sqrt{2I - x^2 - y^2}} - \frac{fxy\sin 3\varphi}{\sqrt{2I - x^2 - y^2}} = \frac{\partial H_1}{\partial I}, \tag{27d}$$

$$H_0(x,y,I,\varphi) = \frac{3}{2}I^2 - sI - \frac{1}{2}y^2(2I - x^2 - y^2) - \frac{b}{2}(x^2 + y^2), \tag{28a}$$

$$H_1(x,y,I,\varphi) = f\sqrt{2I - x^2 - y^2}[(I - y^2)\cos 3\varphi - xy\sin 3\varphi]. \tag{28b}$$

3. The unperturbed system

First, we examine the dynamics of the unperturbed system. Setting $\varepsilon = 0$ in Eq. (26) yields the following set of completely integrable equations describing the unperturbed system as follows:

$$\dot{x} = y(b + 2I - x^2 - 2y^2), \quad \dot{y} = x(-b + y^2), \tag{29a,b}$$

$$\dot{I} = 0, \quad \dot{\varphi} = 3I - s - y^2. \tag{29c,d}$$

We observe that Eq. (29a) and (29b) are completely independent of φ, and $I =$ constant. Thus, we need to study the phase flow in (x,y) phase space only. We recall from Eq. (20) that $p_1 < p_2$ and thus we are interested in the behavior of our system inside the circle described by the following equation:

$$x^2 + y^2 \leqslant 2I. \tag{30}$$

It is observed that since in view of Eq. (25) $(x^2 + y^2)/2 = a_1$, the equality holds when $a_2 = 0$. In other words inequality (30) is nothing more than $a_2 \geqslant 0$.

In phase space (x,y), we are interested in the flow inside a circle whose radius is $\sqrt{2I}$. In Eqs. (29a) and (29b), all possible fixed points ($\dot{x} = \dot{y} = 0$) are

$$\begin{aligned} &\text{I}: \quad x = 0, \quad y = 0, \\ &\text{II}: \quad x = 0, \quad y = \pm\sqrt{I - I_1}, \\ &\text{III}: \quad x = \pm\sqrt{2(I + I_1)}, \quad y = \pm\sqrt{b}, \end{aligned} \tag{31}$$

where $I_1 = -b/2$.

In case of $b < 0$, when $0 < I < I_1$, the origin is the only fixed point (case I) which is a center. At $I = I_1$ a pitchfork bifurcation occurs at the origin generating a saddle at the origin and two centers (case II). In case of $b > 0$, when $0 < I < -I_1$, there exist a center at the origin (case I) and two saddles (case II). At $I = -I_1$, each of the saddles bifurcates into two centers (case III) on a circle $x^2 + y^2 = 2I$.

The bifurcation diagram in the I–b space, of the unperturbed system (29) is shown in Fig. 2. Three bifurcation lines denoted by thick solid lines and the types of fixed points are shown in the figure. Subscripts c and s represent center and saddle, respectively. The bifurcation diagrams in the x–y–I space, of the unperturbed system (29) are shown in Fig. 3. The phase portraits in the x–y space, in Fig. 4, of the unperturbed system (29) reflect the bifurcation diagrams in Fig. 3. In Fig. 4, thick lines denote the circles $x^2 + y^2 = 2I$, on which $a_2 = 0$. In this paper, we are interested in a homoclinic orbit B_I in Fig. 4 (a–1), corresponding to the case of $b < 0$ and $I > I_1$. The origin is connected to itself by a pair of symmetric homoclinic orbits, each of which is described by

$$b(x^2 + y^2) + y^2(2I - x^2 - y^2) = 0. \tag{32}$$

In four-dimensional space $(x$–y–I–$\varphi)$, there exist two-dimensional invariant manifold M_0 and three-dimensional homoclinic manifold Γ, respectively, which are given as

$$M_0 = \{(x, y, I, \varphi) | x = 0, y = 0, I > I_1, \varphi \in T^1\}, \tag{33}$$

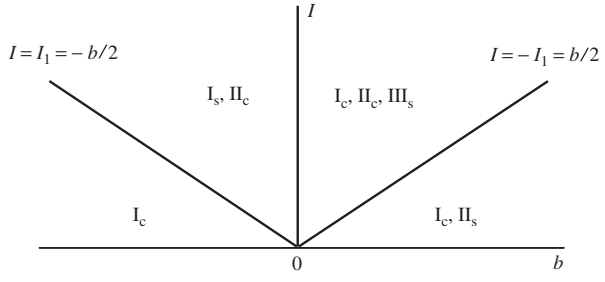

Fig. 2. Bifurcation diagram in the I–b space, of the unperturbed system (29).

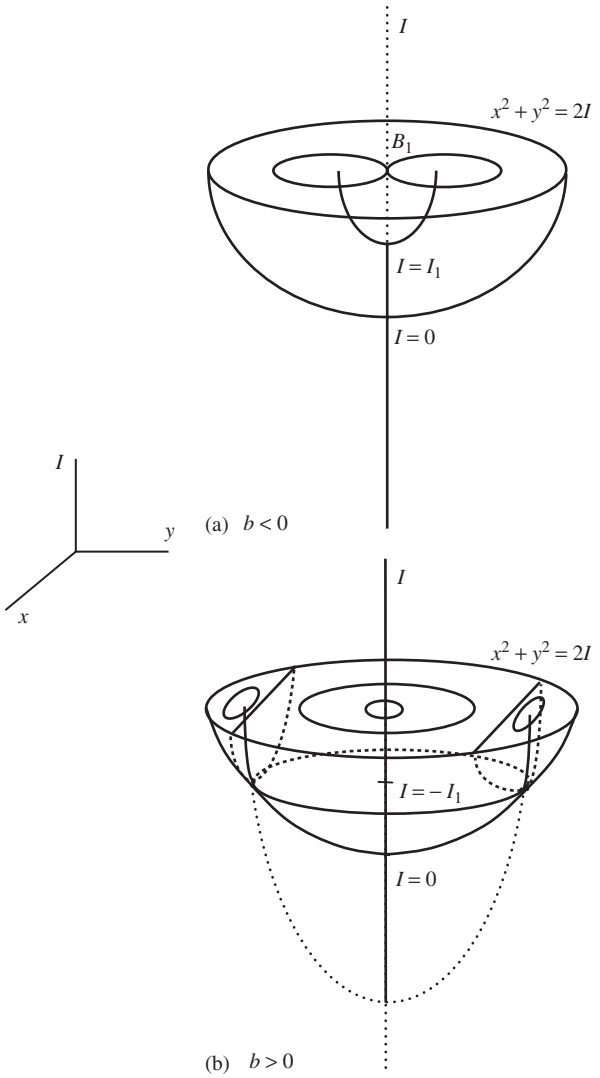

Fig. 3. Bifurcation diagrams in the x–y–I space, of the unperturbed system (29).

$$\begin{aligned} \Gamma = \{(x, y, I, \varphi) | x = x^h(t, I), y = y^h(t, I), I > I_1, \\ \varphi = \textstyle\int_0^t D_1 H_0(x^h(s, I), y^h(s, I), I)\, \mathrm{d}s + \varphi_0\}, \end{aligned} \tag{34}$$

where $(x^h(s, I), y^h(s, I))$ give time parametrization of the homoclinic orbit. Any trajectory on Γ approach M_0 as $t \to \pm\infty$, and $\varphi_0 \in T^1$ (one-dimensional tours) is a constant, which is determined from the initial conditions.

In Eqs. (29c) and (29d) the dynamics restricted to the invariant manifold M_0 is described as follows:

$$\dot{I} = 0, \quad \dot{\varphi} = 3I - s. \tag{35a,b}$$

Since $x = y = 0$ means $a_1 = 0$, the dynamics on M_0 designate a standing wave by the sine mode. Since the unperturbed system has no excitation i.e. $\Lambda = 0$ in Eq. (16b), the response of sine mode x_{20} becomes $A_2(T_1)\exp(\mathrm{i}\omega_2 T_0) + \mathrm{cc}$. Using Eqs. (18)–(20), (22) and (25) we have

$$x_{20}(t) = 2\sqrt{2a_2}\,\cos[\omega_2 T_0 + (\sigma/3)T_1 + \varphi].$$

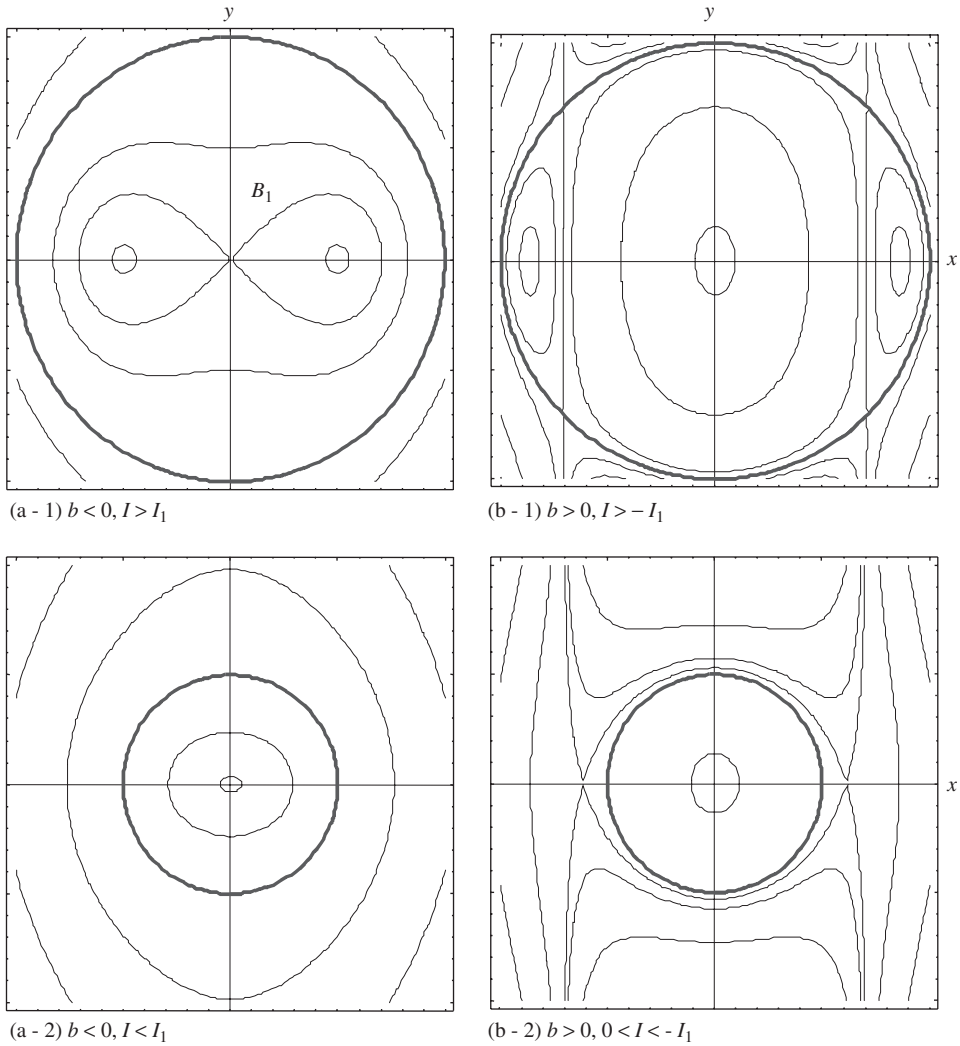

Fig. 4. Phase portraits in the $x-y$ space, of the unperturbed system (29).

Integrating Eq. (35b) with respect to τ we can get $\varphi = (3I - s)\tau + \varphi_0$, where φ_0 is an integrating constant. Transforming s and τ, respectively, into σ and εt via Eq. (22), we have a steady state periodic response

$$x_{20}(t) = 2\sqrt{2I}\cos[\omega_2(1 + 3\varepsilon\gamma I)t + \varphi_0],$$

whose frequency $\omega_2(1 + 3\varepsilon\gamma I)$ is shown to depend on the energy level I determining the amplitude of the response. This tendency implies that the cubic nonlinearity of the system has the characteristic of a hardening spring.

In Eqs. (35), we can see that $\dot{\varphi} = 0$ for $I = I_r$, where $I_r = s/3$. This value is called the resonant value of I. The case of $I = I_r$ corresponds to the circle of fixed points in (I,φ) plane. The cases of $I \neq I_r$ correspond to the circles, which are periodic orbits in (I,φ) plane. These circles are shown in Fig. 5. Since $I_r > I_1$ we can see the relationship as follows:

$$s > -\frac{3}{2}b. \tag{36}$$

If a particle starts marching along the homoclinic orbit, an infinite amount of time is required by the particle to return to the saddle point itself. During this time, in view of Eq. (35) φ may change by an infinite amount

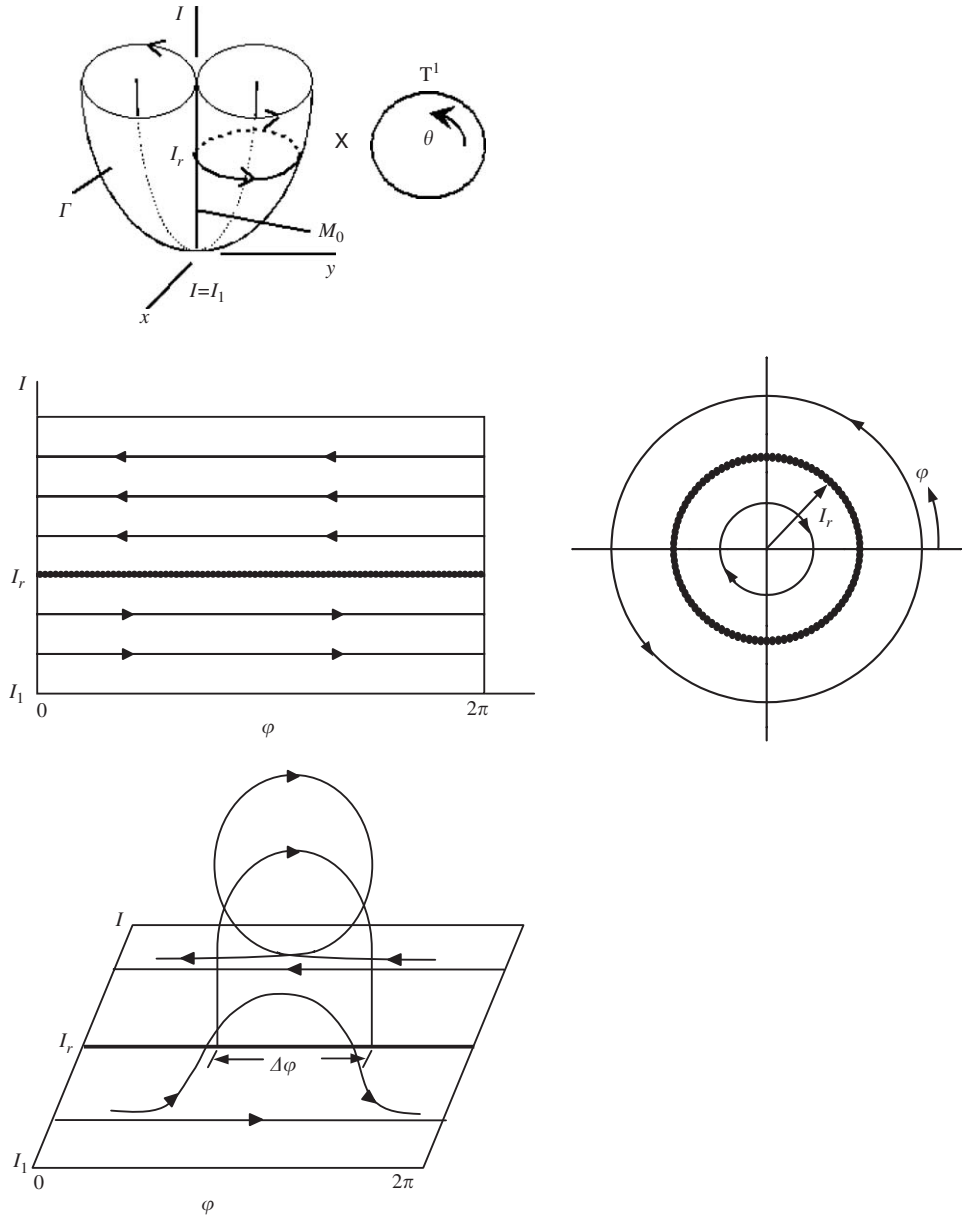

Fig. 5. Flow in (I,φ) plane at $x = y = 0$.

when $I \neq I_r$. However, if $I = I_r$, φ changes by a finite amount:

$$\Delta\varphi \equiv \varphi(\infty, I_r) - \varphi(-\infty, I_r). \tag{37}$$

This value is called phase shift. In order to calculate $\Delta\varphi$, we need an expression for the homoclinic orbit at $I = I_r$. For convenience, we use the coordinate system (p_1, q_1), which is a polar coordinate system corresponding to the rectangular coordinate system (x,y). In Eqs. (21a) and (21b), consider $\varepsilon = 0$.

$$\dot{p}_1 = 2p_1(I_r - p_1)\sin 2q_1 = -\frac{\partial \bar{H}}{\partial q_1}, \tag{38a}$$

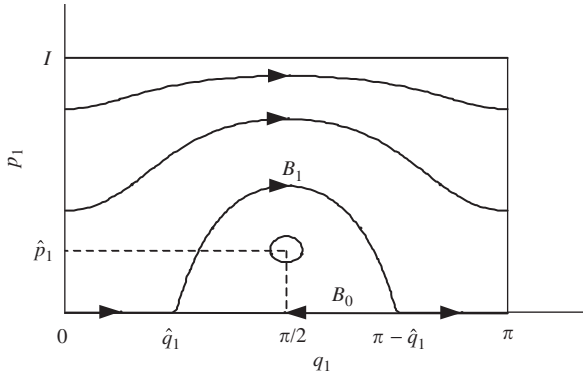

Fig. 6. Phase portraits in (p_1, q_1) plane when $I > I_1$.

$$\dot{q}_1 = -b - (I_r - 2p_1)(1 - \cos 2q_1) = \frac{\partial \bar{H}}{\partial p_1}, \tag{38b}$$

where

$$\bar{H}(p_1, q_1) = -bp_1 - p_1(I_r - p_1)(1 - \cos 2q_1). \tag{39}$$

Since system (38) is periodic with period π in q_1, we consider the range of q_1 from 0 to π. Then in Eq. (38), fixed points are given as

$$\text{center}: \quad (\hat{p}_1, \pi/2) \quad \text{saddles}: \quad (0, \hat{q}_1), \quad (0, \pi - \hat{q}_1), \tag{40}$$

where

$$\hat{p}_1 = \frac{1}{4}(2I_r + b), \quad \hat{q}_1 = \frac{1}{2}\cos^{-1}\left(1 + \frac{b}{I_r}\right). \tag{41a,b}$$

The homoclinic orbit B_1 in rectangular coordinate system (x,y) corresponds to the heteroclinic orbit B_1 in coordinate system (p_1,q_1) shown in Fig. 6. On the heteroclinic orbit B_1 we have

$$q_1(-\infty) = \hat{q}_1 \quad \text{when} \quad t \to -\infty \tag{42a}$$

and

$$q_1(\infty) = \pi - \hat{q}_1 \quad \text{when} \quad t \to \infty. \tag{42b}$$

In Eq. (39), this heteroclinic orbit B_1 on which $\bar{H}(p_1, q_1)$ can be obtained from $\bar{H}(0, \hat{q}_1)$, is given as

$$p_1 = I_r + \frac{b}{1 - \cos 2q_1}. \tag{43}$$

Setting $\varepsilon = 0$ and $I = I_r$ in Eq. (21d), adding the result and Eq. (38b), and substituting Eq. (43) into the result, we obtain $\dot{q}_1 + \dot{q}_2 = 0$, which gives $q_1 + q_2 = C_0$, a constant. In view of Eq. (25) we have the relation $\theta(t, I_r) = C_0 - q_1(t)$. Then phase shift defined in Eq. (37) is calculated by Eq. (42) as follows:

$$\Delta\varphi = -q_1(\infty) + q_1(-\infty) = 2\hat{q}_1 - \pi. \tag{44}$$

4. The perturbed system

From Eqs. (26a,b) and (27a,b) we can see that subspace $x = y = 0$ is invariant even when $\varepsilon \neq 0$. Under perturbation (when $\varepsilon \neq 0$), M_0 becomes a locally invariant two-dimensional manifold M_ε described as follows:

$$\begin{aligned} M_\varepsilon = \{&(x_\varepsilon, y_\varepsilon, I, \varphi) | x_\varepsilon(I, \varphi) = 0 + \varepsilon x_1(I, \varphi) + O(\varepsilon^2), \\ &y_\varepsilon(I, \varphi) = 0 + \varepsilon y_1(I, \varphi) + O(\varepsilon^2), I > I_1, \varphi \in T^1\}. \end{aligned} \tag{45}$$

Substituting x_ε and y_ε into Eqs. (26c) and (26d), respectively, we have the flow on M_ε as follows:

$$\dot{I} = \varepsilon(-2cI + 3\sqrt{2}fI^{3/2}\sin 3\varphi) + O(\varepsilon^3), \tag{46a}$$

$$\dot{\varphi} = 3I - s + \varepsilon\frac{3f}{\sqrt{2}}\sqrt{I}\cos 3\varphi + O(\varepsilon^2). \tag{46b}$$

In order to examine the dynamics of invariant manifold M_ε in the neighborhood of $I = I_r$, we introduce the rescaling

$$I = I_r + \sqrt{\varepsilon}h, \quad \tau = \tilde{\tau}/\sqrt{\varepsilon}, \tag{47}$$

where $\tilde{\tau}$ represents another slow time. The flow on M_ε is described as

$$h' = -3\sqrt{2}fI_r^{3/2}(K_1 - \sin 3\varphi) + \sqrt{\varepsilon}G(h,\varphi) + O(\varepsilon), \tag{48a}$$

$$\varphi' = 3h + \sqrt{\varepsilon}F(h,\varphi) + O(\varepsilon), \tag{48b}$$

where

$$K_1 = \frac{\sqrt{2}c}{3f\sqrt{I_r}}, \quad F(h,\varphi) = \frac{3f\sqrt{I_r}}{\sqrt{2}}\cos 3\varphi, \quad G(h,\varphi) = -\frac{3f\sqrt{I_r}}{\sqrt{2}}h(2K_1 - 3\sin 3\varphi)$$

and a prime denotes differentiation with respect to $\tilde{\tau}$.

When $\varepsilon = 0$, Eq. (46) is a Hamiltonian system with Hamiltonian function

$$L(h,\varphi) = \frac{3}{2}h^2 + \sqrt{2}fI_r^{3/2}(3K_1\varphi + \cos 3\varphi). \tag{49}$$

Fig. 7 shows two fixed points of the Hamiltonian system ($h' = -L_\varphi$ and $\theta' = L_h$) as follows:

$$\text{center}: \quad p_0 = (0,\varphi_c) \quad \text{saddle}: \quad q_0 = (0,\varphi_s), \tag{50}$$

where $\varphi_s = (1/3)\sin^{-1}K_1$ and $\varphi_c = (1/3)(\pi - \sin^{-1}K_1)$. Since value of non-dimensionalized parameter K_1 must be in the domain of arcsine function, condition $|K_1| \leqslant 1$ should be satisfied. Since the Hamiltonian system is periodic in φ of $2\pi/3$ we only consider the range of $0 < \varphi < 2\pi/3$. Under perturbation saddle points q_0 and q_ε become center p_0 and sink p_ε, respectively. A shaded region in Fig. 7(a) is an approximation of domain of attraction of sink p_ε in Fig. 7(b). The region is enclosed by the homoclinic orbit connecting the unstable fixed point q_0 to itself. The level of Hamiltonian function on the orbit is equal to $L(0,\varphi_s)$.

Let us consider the dynamics on M_ε, in the neighborhood of I_r defined as an annulus:

$$A_\varepsilon = \{(x,y,h,\varphi)|x = 0, \ \ y = 0, \ \ |h| < \varepsilon C, \ \ \varphi \in T^1\}, \tag{51}$$

where $C > 0$ is a constant, chosen sufficiently large as to enclose the unperturbed homoclinic orbit within it.

Contrary to unperturbed system, where $x = y = 0$ means that the response of sine mode x_{20} becomes $A_2(T_1)\exp(\mathrm{i}\omega_2 T_0) + \mathrm{cc}$, in perturbed system $x = y = 0$ means that the response consists of resonance and non-resonance ones having frequencies ω_2 and λ, respectively, as shown in Eq. (16b). Since $x = y = 0$ means $a_1 = 0$, the dynamics on A_ε designates a standing wave having two frequencies ω_2 and λ.

Fig. 7(b) shows a transformation of this annulus A_ε being a small segment of the perturbed invariant manifold M_ε. The stable and unstable three-dimensional manifolds of A_ε, respectively, denoted as $W^s(A_\varepsilon)$ and $W^u(A_\varepsilon)$, are the subsets of $W^s(M_\varepsilon)$ and $W^u(M_\varepsilon)$. For some parameter values, an orbit that leaves p_ε while coming out of the annulus A_ε in four-dimensional phase space, may return to the annulus and eventually complete a Silnikov-type homoclinic orbit shown in Fig. 8. The figure shows that the orbit left A_ε returns to itself. Speaking in terms of responses of circular plate, we may say that the orbit implies a motion starting from a standing wave returns to the standing wave thru a traveling wave. Contrary to the standing wave given by the sine mode only, in view of Eq. (3), the traveling wave consists of not only the sine mode but also the cosine mode.

The existence of such an orbit connecting the saddle focus p_ε is examined in two steps. In the first step, using higher-dimensional Melnikov theory, one obtains condition for $W^u(p_\varepsilon) \cap W^s(A_\varepsilon) \neq \varnothing$, i.e. when a trajectory

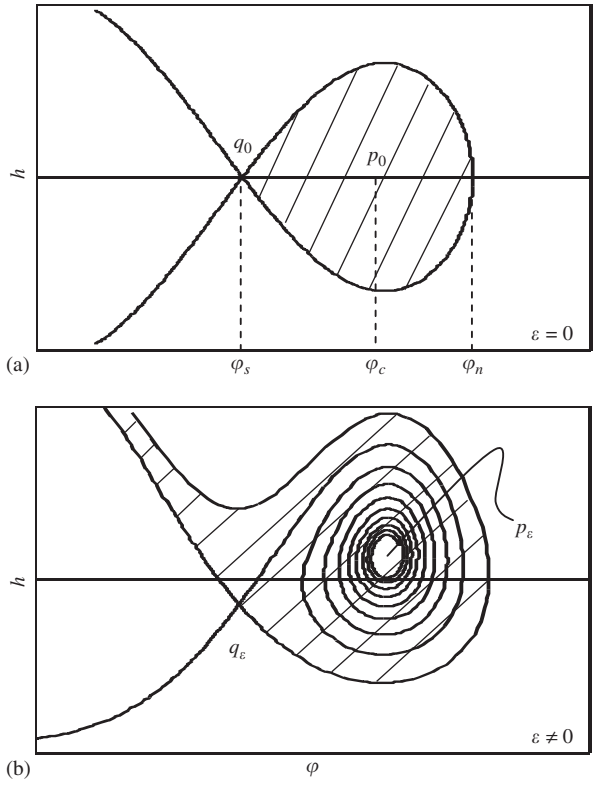

Fig. 7. Dynamics on (I,φ) plane in the neighborhood of $I = I_r$ for $x = y = 0$.

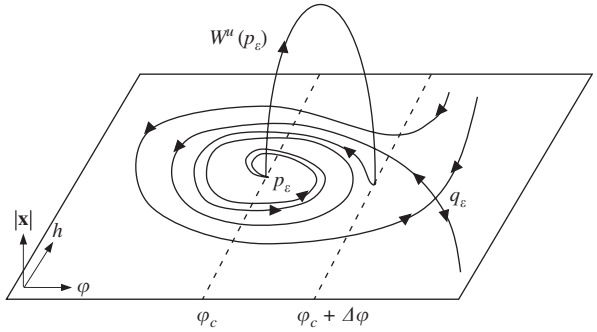

Fig. 8. Silnikov-type homoclinic orbit to p_ε.

leaving p_ε comes back in the neighborhood of A_ε. In the second step, we have to examine whether this orbit (in $W^u(p_\varepsilon)$) comes back in the domain of attraction of p_ε [17,21].

In order to begin the first step we evaluate the Melnikov function, which gives a measure of the distance between two manifolds, $W^u(p_\varepsilon)$ and $W^s(A_\varepsilon)$. The condition $W^u(p_\varepsilon) \cap W^s(A_\varepsilon) \neq \varnothing$ is satisfied when the Melnikov function is equal to zero [18]. It is computed in the following manner [1,24,25]:

$$M^{I_r} = \int_{-\infty}^{\infty} \left[\frac{\partial H_0}{\partial x} g^x + \frac{\partial H_0}{\partial y} g^y + \frac{\partial H_0}{\partial I} g^I \right] \mathrm{d}t, \tag{52}$$

where the integrand has been evaluated at any arbitrary point on Γ at $I = I_r$. Functions H_0, g^x, g^y and g^I are given in Eq. (27). After some calculations we can express the Melnikov function as follows:

$$M^{I_r} = -[H_1(\infty) - H_1(-\infty)] - b\int_{-\infty}^{\infty}[c + \gamma b(b + 3I_r)\cot\, q_1](\csc q_1^2)\dot{q}_1\,\mathrm{d}t, \tag{53}$$

where $H_1(\infty)$ and $H_1(-\infty)$ denote $H_1(x, y, I_r, \varphi)$ when $t \to \infty$ and $t \to -\infty$, respectively. We can observe that $\varphi \to \varphi_c + \Delta\varphi$ and $\varphi \to \varphi_c$, respectively, as $t \to \infty$ and $t \to -\infty$, and that $(x, y) \to (0, 0)$ as $t \to \pm\infty$. Therefore, $H_1(\infty) = H_1(0, 0, I_r, \varphi_c + \Delta\varphi)$ and $H_1(-\infty) = H_1(0, 0, I_r, \varphi_c)$. In view of Eqs. (28b) and (42), Melnikov function (53) is reduced as follows:

$$\begin{aligned} M^{I_r} &= \sqrt{2}fI_r^{3/2}[\cos\, 3\varphi_c - \cos\, 3(\varphi_c + \Delta\varphi)] \\ &\quad - b\int_{\hat{q}}^{\pi-\hat{q}_1}[c + \gamma b(b + 3I_r)\cot\, q_1]\csc q_1^2\,\mathrm{d}q_1 \\ &= \sqrt{2}fI_r^{3/2}[\cos\, 3\varphi_c - \cos\, 3(\varphi_c + \Delta\varphi)] - 2bc\,\cot\,\hat{q}_1. \end{aligned} \tag{54}$$

In view of Eqs. (41b) and (44) and the expression of φ_c in Eq. (50), we can see that when the Melnikov function vanishes the value of K_1 becomes

$$K_1^M = \frac{(1 + 2K_2)^2}{\sqrt{1 + 8K_2 + 24K_2^2}}, \tag{55}$$

where $K_2 = b/I_r$. In derivation of Eq. (55) a negative sign of K_1^M has been neglected, since c and f are positive. Since $I_r > I_1 > -b/2$, we have $-2 < K_2 < 0$.

In order to begin the second step we have to check whether the unstable manifold of p_ε has a change of angle $\Delta\varphi$ such that it lies in the domain of attraction in A_ε of p_ε (see Figs. 7 and 8). The condition is

$$\varphi_s < \varphi_c + \Delta\varphi + 2m\pi/3 < \varphi_n, \quad m \in \text{Integer}, \tag{56}$$

where φ_s and φ_c are defined in Eq. (50). Hamiltonian function remains constant on the homoclinic orbit, that is, we can use relation $L(0, \varphi_n) = L(0, \varphi_s)$. The relation is finally reduced to

$$\sqrt{2}fI_r^{3/2}[3K_1(\varphi_n - \varphi_s) + \cos\, 3\varphi_n - \cos\, 3\varphi_s] = 0. \tag{57}$$

Using $fI_r \neq 0$ and Eq. (50) we can reduce Eq. (57) to

$$-\sqrt{1 - K_1^2} + 3K_1\varphi_n - K_1\sin^{-1}K_1 + \cos\, 3\varphi_n = 0 \tag{58}$$

from which φ_n can be obtained. In view of Eqs. (50) and (58) we come to know that φ_s, φ_c and φ_n are given by K_1. Identifying K_1 with K_1^M and noting that

$$\Delta\varphi = \cos^{-1}(1 + K_2) - \pi, \tag{44′}$$

we would like to determine values of parameters K_1 and K_2 satisfying two conditions. Now φ_s, φ_c, φ_n and $\varphi_c + \Delta\varphi$ are represented as functions of K_2 via Eq. (55). The first three are denoted by thin lines and the last by thick lines in Fig. 9. In the figure thick and solid line denotes the region $(-1.0328 = K_2^1 < K_2 < K_2^2 = -0.1667)$ where two conditions for the existence of Silnikov-type homoclinic orbit are satisfied. In view of Eq. (55) $K_2 = K_2^1$ and K_2^2 are corresponding to $K_1 = K_1^{M1} = 0.2652$ and $K_1^{M2} = 0.7698$, respectively, as shown in Fig. 10. Taking $b = -0.2868$, we have an interval $0.833075 < s < 5.16137$ corresponding to the interval $-1.0328 < K_2 = 3b/s < -0.1667$. Fig. 11 shows a surface representing a set of values of c, f and s, on which two conditions (55) and (56) are satisfied, when $b = -0.2868$. In order to seek Silnikov-type homoclinic orbit or strange attractor with Smale horseshoe structure we integrated numerically Eq. (26) with many combinations of parameter values and initial conditions. Fig. 12 shows a typical long-term behavior, which is a periodic orbit obtained numerically by taking $\varepsilon = 0.001$, $K_1 = 0.402235$, $K_2 = -0.239$, $\gamma = 3.787$ $s = 3.6$, $f = 0.891$, $c = 0.832827$, $b = -0.2868$, $x(0) = 0.419643 \times 10^{-8}$, $y(0) = 0.154596 \times 10^{-8}$, $I(0) = 1.20063$, $\theta(0) = 0.90925$. In spite of all efforts, neither Silnikov-type homoclinic orbit nor strange attractor with Smale horseshoe structure has been found, which is a remarkable contrast to what those had been reported to

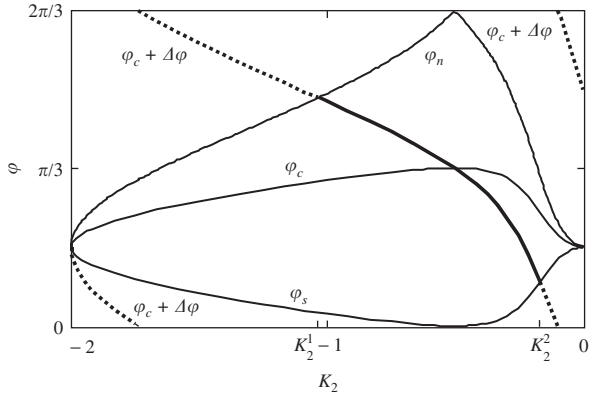

Fig. 9. Plot of $\varphi_c + \Delta\varphi$ as a function of K_2.

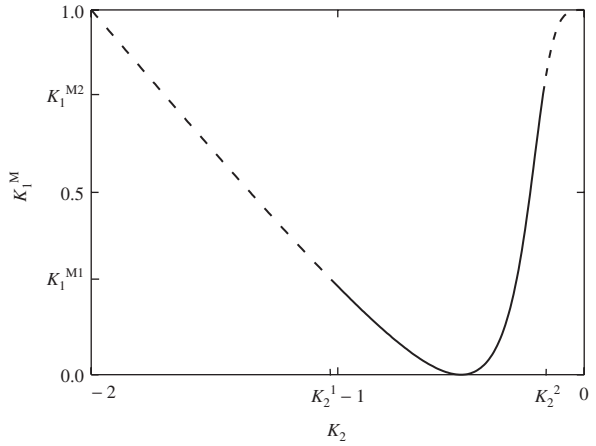

Fig. 10. Plot of K_1^M as a function of K_2 as the condition for $M^{I_r} = 0$.

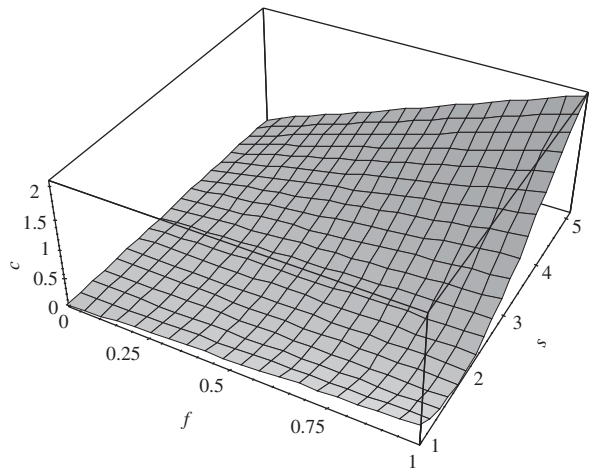

Fig. 11. A surface in the parameter space on which two conditions (55) and (56) for $b = -0.2868$ are satisfied.

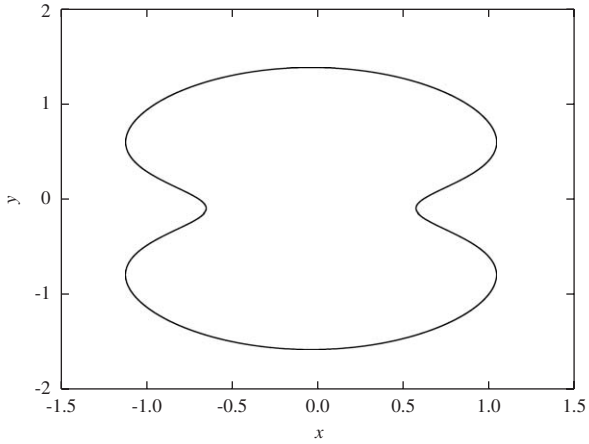

Fig. 12. A periodic motion in (x, y) plane for $\varepsilon = 0.001$, $K_1 = 0.402235$, $K_2 = -0.239$, $\gamma = 3.787$, $x(0) = 0.419643 \times 10^{-8}$, $y(0) = 0.154596 \times 10^{-8}$, $I(0) = 1.20063$ and $\theta(0) = 0.90925$.

be obtained numerically by Feng and his colleagues [18,22]. Unravelling the reason why we have failed to observe any numerical evidences of global bifurcation result obtained by Kovačič and Wiggins' method [17] is beyond the scope of the work. We can, however, only conjecture on the reason in two ways. First, the system is so sensitive to values of parameters that the first order of approximation (26) may not be good enough for the global bifurcation. Second, the homoclinic orbit and the strange attractor are so sensitive to initial conditions, which means that we might not have tried enough number of initial conditions to find those. Further study is needed.

5. Conclusion

The global bifurcations in modal interactions of an imperfect circular plate with one-to-one internal resonance are investigated. The case of the third-order subharmonic resonance, in which an excitation frequency is near triple natural frequencies, is considered. The equations governing nonlinear oscillations of an imperfect circular plate are reduced to a system of non-autonomous ordinary differential equations via Galerkin's procedure. The method of multiple scales is used to obtain a system of autonomous ordinary differential equations, and then Kovačič and Wiggins' method is used to investigate the global dynamics of the plate. Having found a region of parameters where a sufficient condition for the existence of Silnikov-type homoclinic orbit is satisfied, we failed to observe any numerical evidences of global bifurcation.

Acknowledgment

This research was supported by the Korea Science and Engineering Foundation under Grant No. R01-2000-000-00289-0.

References

[1] S. Wiggins, *Global Bifurcations and Chaos: Analytical Methods*, Springer, New York Inc., 1988.
[2] S.I. Chang, A.K. Bajaj, C.M. Krousgill, Non-linear vibrations and chaos in harmonically excited rectangular plates with one-to-one internal resonance, *Non-linear Dynamics* 4 (1993) 433–460.
[3] G.J. Efstathiades, A new approach to the large-deflection vibrations of imperfect circular disks using Galerkin's procedure, *Journal of Sound and Vibration* 16 (1971) 231–253.
[4] S. Sridhar, D.T. Mook, A.H. Nayfeh, Non-linear resonances in the forced responses of plates, part I: symmetric responses of circular plates, *Journal of Sound and Vibration* 41 (1975) 359–373.
[5] J. Hadian, A.H. Nayfeh, Modal interaction in circular plates, *Journal of Sound and Vibration* 142 (1990) 279–292.

[6] W.K. Lee, C.H. Kim, Combination resonances of a circular plate with three-mode interaction, *American Society of Mechanical Engineers Journal of Applied Mechanics* 62 (1995) 1015–1022.
[7] S. Sridhar, D.T. Mook, A.H. Nayfeh, Non-linear resonances in the forced responses of plates, part II: asymmetric responses of circular plates, *Journal of Sound and Vibration* 59 (1978) 159–170.
[8] T.A. Nayfeh, A.F. Vakakis, Subharmonic traveling waves in a geometrically non-linear circular plate, *International Journal of Non-linear Mechanics* 29 (1994) 233–245.
[9] M.H. Yeo, W.K. Lee, Corrected solvability conditions for non-linear asymmetric vibrations of a circular plate, *Journal of Sound and Vibration* 257 (2002) 653–665.
[10] W.K. Lee, M.H. Yeo, Non-linear interactions in asymmetric vibrations of a circular plate, *Journal of Sound and Vibration* 263 (2003) 1017–1030.
[11] W.K. Lee, M.H. Yeo, S.B. Samoilenko, The effect of the number of the nodal diameters on non-linear interactions in two asymmetric vibration modes of a circular plate, *Journal of Sound and Vibration* 268 (2003) 1013–1023.
[12] C. Touzé, O. Thomas, A. Chaigne, Asymmetric non-linear forced vibrations of free-edge circular plates. Part I: theory, *Journal of Sound and Vibration* 258 (2002) 649–676.
[13] O. Thomas, C. Touzé, A. Chaigne, Asymmetric non-linear forced vibrations of free-edge circular plates. Part II: experiments, *Journal of Sound and Vibration* 265 (2003) 1075–1101.
[14] Z.C. Feng, P.R. Sethna, Global bifurcation and chaos in parametrically forced systems with one–one resonance, *Dynamics and Stability of Systems* 5 (1990) 201–225.
[15] X.L. Yang, P.R. Sethna, Local and global bifurcations in the parametrically excited vibrations of nearly square plate, *International Journal of Non-linear Mechanics* 26 (1991) 199–220.
[16] X.L. Yang, P.R. Sethna, Non-linear phenomena in forced vibrations of a nearly square plate: antisymmetric case, *Journal of Sound and Vibration* 155 (1992) 413–441.
[17] G. Kovačič, S. Wiggins, Orbit homoclinic to resonances, with an application to chaos in a model of the forced and damped Sine-Gordon equation, *Physica D* 57 (1992) 185–225.
[18] Z.C. Feng, P.R. Sethna, Global bifurcations in the motion of parametrically excited thin plates, *Nonlinear Dynamics* 4 (1993) 389–408.
[19] W.-M. Tien, N. Sri Namachchivaya, A.K. Bajaj, Non-linear dynamics of a shallow arch under periodic excitation—I. 1:2 internal resonance, *International Journal of Non-linear Mechanics* 29 (1994) 349–366.
[20] W.-M. Tien, N. Sri Namachchivaya, N. Malhotra, Non-linear dynamics of a shallow arch under periodic excitation—II. 1:1 internal resonance, *International Journal of Non-linear Mechanics* 29 (1994) 367–389.
[21] N. Malhotra, N. Sri Namachchivaya, Global bifurcations in externally excited two-degree-of-freedom nonlinear systems, *Nonlinear Dynamics* 8 (1995) 85–109.
[22] Z.C. Feng, K.M. Liew, Global bifurcations in parametrically excited systems with zero-to-one internal resonance, *Nonlinear Dynamics* 21 (2000) 249–263.
[23] A.H. Nayfeh, D.T. Mook, *Nonlinear Oscillations*, Wiley, New York, 1979.
[24] J. Guckenheimer, P. Holmes, *Nonlinear Oscillations, Dynamical Systems, and Bifurcations of Vector Fields*, Springer, New York Inc., 1983.
[25] S. Wiggins, *Introduction to Applied Nonlinear Dynamical Systems and Chaos*, Springer, New York Inc., 1990.